HHS Public Access

Author manuscript

Curr Biol. Author manuscript; available in PMC 2016 November 02.

Published in final edited form as:

Curr Biol. 2015 November 2; 25(21): 2763–2773. doi:10.1016/j.cub.2015.09.018.

All spiking, sustained ON displaced amacrine cells receive gap-junction input from melanopsin ganglion cells

Aaron N. Reifler[1,3], **Andrew P. Chervenak**[1,3], **Michael E. Dolikian**[1,3], **Brian A. Benenati**[1], **Benjamin Y. Li**[1], **Rebecca D. Wachter**[1], **Andrew M. Lynch**[1], **Zachary D. Demertzis**[1], **Benjamin S. Meyers**[1], **Fady S. Abufarha**[1], **Elizabeth R. Jaeckel**[1], **Michael P. Flannery**[1], and **Kwoon Y. Wong**[1,2,4]

[1]Department of Ophthalmology & Visual Sciences, University of Michigan, Ann Arbor, MI 48105

[2]Department of Molecular, Cellular & Developmental Biology, University of Michigan, Ann Arbor, MI 48105

SUMMARY

Retinal neurons exhibit sustained *vs.* transient light responses, which are thought to encode low- and high-frequency stimuli respectively. This dichotomy has been recognized since the earliest intracellular recordings from the 1960s, but the underlying mechanisms are not yet fully understood. We report that in the ganglion cell layer of rat retinas, all spiking amacrine interneurons with sustained ON photoresponses receive gap-junction input from intrinsically photosensitive retinal ganglion cells (ipRGCs), recently discovered photoreceptors that specialize in prolonged irradiance detection. We have identified three morphological varieties of such ipRGC-driven displaced amacrine cells: *1)* monostratified cells with dendrites terminating exclusively in sublamina S5 of the inner plexiform layer; *2)* bistratified cells with dendrites in both S1 and S5; and *3)* polyaxonal cells with dendrites and axons stratifying in S5. Most of these amacrine cells are wide-field, although some are medium-field. The three classes respond to light differently, suggesting they probably perform diverse functions. These results demonstrate that ipRGCs are a major source of tonic visual information within the retina and exert widespread intraretinal influence. They also add to recent evidence that ganglion cells signal not only to the brain.

[4]Correspondence: kwoon@umich.edu.
[3]Equal contribution.

AUTHOR CONTRIBUTIONS

K.Y.W. conceived this project, did all immunostaining and confocal microscopy, and wrote the manuscript. All 13 authors performed whole-cell recordings, with A.N.R., A.P.C. and M.E.D. contributing the most data. A.N.R., A.P.C. and K.Y.W. analyzed the data and made the figures.

INTRODUCTION

Vision begins in the retina, where multiple stimulus attributes are processed in parallel. For example, the >10 types of bipolar cells, >30 types of amacrine cells and >20 types of ganglion cells are divided into ON and OFF varieties, signaling increments and decrements in light intensity respectively. Moreover, both ON and OFF neurons are further divided into transient *vs.* sustained types to encode different temporal information [1]. Significant effort has been made to elucidate the mechanisms shaping a cell's photoresponse kinetics. For amacrine cells, transient photoresponses may be produced by inhibitory feedback to presynaptic bipolar cells [2], the use of NMDA-type glutamate receptors [3], and rapid desensitization of ionotropic glutamate receptors [4]. Conversely, sustained amacrine photoresponses have been correlated with the presence of AMPA-type glutamate receptors [3], certain voltage-dependent conductances [2], and, most pertinent to the present study, excitatory input from intrinsically photosensitive retinal ganglion cells (ipRGCs) [5].

ipRGCs are inner retinal photoreceptors that contain the photopigment melanopsin and mediate irradiance-dependent visual functions such as pupillary constriction, circadian photoentrainment, and brightness discrimination [6, 7]. Though ipRGCs are directly light-sensitive, they also receive synaptic input and generate rod/cone-driven photoresponses. Both their melanopsin-based and rod/cone-driven light responses are depolarizing and far more tonic than the light responses of all other ganglion cells [8]. ipRGCs signal not only to the brain but also to about a third of the dopaminergic amacrine (DA) cells [5], through which ipRGCs might regulate dopamine secretion [9]. ipRGC-driven DA cells exhibit sustained excitatory photoresponses that survive pharmacological block of ON bipolar cell signaling but are abolished by AMPA/kainate receptor antagonism, indicating they respond to ipRGC input via ionotropic glutamate receptors. By contrast, the remaining DA cells, which do not get ipRGC input, generate transient light responses mediated by ON bipolar cells [5].

Intraretinal signaling by ipRGCs could extend beyond DA cells because a recent study revealed tracer coupling between ipRGCs and some amacrine cells displaced to the ganglion cell layer (GCL) [10]. Because tracer coupling implies the presence of gap junctions and gap junctions form sign-preserving electrical synapses, coupling between ipRGCs and displaced amacrines could allow the former to transmit their tonic depolarizing light responses to the latter, which would represent a novel mechanism for producing sustained photoresponses in amacrine cells. We tested this hypothesis here.

RESULTS

Overview

This was part of a 5-year project searching for ipRGCs and ipRGC-driven displaced amacrine cells in rat retinas. We whole-cell-recorded from ~3,900 randomly selected somas in the GCL of Sprague Dawley rat eyecups, presented a 10-s full-field 480-nm light step to each neuron, and studied those exhibiting a purely depolarizing response throughout the stimulus. All other neurons were discarded, including those that depolarized transiently, and those that hyperpolarized either transiently or continuously. When a sustained ON cell was

found, rod/cone signaling was blocked using a cocktail of "glutamate blockers" containing 50 μM L-(+)-2-amino-4-phosphonobutyric acid (L-AP4), 40 μM 6,7-dinitroquinoxaline-2,3-dione (DNQX), and 25 μM D-(−)-2-amino-5-phosphonopentanoic acid (D-AP5). 10-s light steps were presented again to probe for rod/cone-independent responses. Intracellular dye fills were analyzed using confocal microscopy to examine the cells' morphologies. All neurons extending an axon toward the retinal surface were categorized as ipRGCs and described elsewhere [11]. The rest were amacrine cells and are discussed in the present communication.

Non-spiking sustained ON amacrine cells lack rod/cone-independent light responses

Early in the project, we encountered many small non-spiking GCL neurons exhibiting sustained ON photoresponses in normal Ames' medium, of which most were starburst cells (Fig. 1A). Without exception, their light responses were eliminated by the abovementioned glutamate-blocking cocktail ($n = 12$) (Fig. 1B), or by L-AP4 alone ($n = 5$), suggesting non-spiking, sustained ON cells respond to light only through rod/cone input. To increase the efficiency of our search for ipRGC-driven amacrine cells, we discarded all subsequently encountered non-spiking sustained ON cells.

All spiking sustained ON amacrine cells generate rod/cone-independent photoresponses

We came across 232 spiking neurons displaying sustained ON photoresponses in normal Ames', of which 154 lacked a superficially projecting axon and were presumed amacrine cells. To verify that the absence of such an axon reliably identifies amacrine cells, 47 of these 154 putative amacrines were randomly picked for immunohistochemistry against the retinal ganglion cell (RGC) marker RBPMS [12], and none were stained (Fig. 2A). Eight additional randomly selected presumed amacrines were tested with an antibody against the amacrine-cell neurotransmitter GABA, and 6 were immunopositive (Fig. 2B).

Remarkably, all 154 spiking sustained ON amacrine cells remained light-sensitive in the presence of the glutamate blockers (Fig. 2C), indicating an ability to respond to light without rod/cone input. Glutamate block altered these cells' photoresponses in three ways: their threshold intensity was elevated by several log units; response onset was delayed; and the transient hyperpolarization often seen at light offset was eliminated (Fig. 2C).

Evidence for input from ipRGCs

During rod/cone signaling block, the sustained displaced amacrine cells' light responses had a striking resemblance to the sluggish melanopsin-based photoresponses of ipRGCs [13]. To test whether these responses originated from ipRGCs, we used the method described in ref. [11] to estimate their λ_{max} and found it to be 478.3±0.8 nm, which was statistically indistinguishable ($p = 0.35$) from the λ_{max} previously measured for ipRGCs' melanopsin-based responses [11]. As additional evidence for ipRGC input, we were able to detect similarly sluggish, melanopsin-like depolarizing photoresponses in 3 displaced amacrine cells in retinally degenerate mouse retinas (Fig. 3B).

Morphological classification

The dye fills of 116 ipRGC-driven amacrines were sufficiently robust to enable detailed examination of their dendritic morphologies, which formed three broad categories. Forty-three cells had dendrites stratifying exclusively in sublamina S5 of the inner plexiform layer (IPL) (Fig. 4A), while 31 cells had dendrites stratifying in S1 and S5 (Fig. 4C). The remaining 42 cells possessed not only dendrites but also several long, relatively straight and thin axons; these polyaxonal amacrines stratified in S5 (Fig. 4E). For all three categories, some distal processes were so fine that it was difficult to judge whether the confocal images captured the entire dendritic/axonal field. In the field size histograms in Fig. 4, the cells that were unequivocally completely imaged are represented by the light columns, whereas those that might not have been fully imaged are indicated by the dark columns. The field sizes within each category spanned a very large range, suggesting that each category likely included multiple cell types (Fig. 4B,D,F).

As mentioned earlier, some DA cells receive ipRGC input [5]. In the Sprague Dawley rat retina, a very small number (<10 per retina) of DA cells are displaced to the GCL [14]. To assess whether our spiking sustained ON amacrines were merely displaced DA cells, we randomly picked 9 cells (2 monostratified, 1 bistratified, and 6 polyaxonal) for immunostaining against the DA cell marker tyrosine hydroxylase. None was labeled (Fig. 4G), indicating they are novel ipRGC-driven cells.

Photoresponse diversity

Fig. 5A–C shows the ipRGC-driven displaced amacrine cells' averaged graded responses, and Fig. 5H–J shows their averaged spiking responses. Because morphological diversity implies functional diversity, we quantified these amacrine cells' light responses and looked for differences among the three classes. For both graded and spiking responses, four properties were quantified: *1)* peak amplitude in normal Ames'; *2)* final-to-peak amplitude ratio in normal Ames', calculated by dividing the response amplitude near the end of the 10-s stimulus by the peak amplitude – this ratio quantifies the "sustainedness" of the response; *3)* peak amplitude during glutamate block; and *4)* latency to peak during glutamate block. No class-dependent differences were found for the peak amplitude of the graded responses, whether measured in the presence of normal Ames' (Fig. 5D) or glutamate blockers (Fig. 5F). For each of the other properties, however, significant differences could be seen between at least two morphological classes. The bistratified and monostratified cells were different in three properties (Fig. 5E,M,N), bistratified and polyaxonal cells in five (Fig. 5E,G,K,L,N), and monostratified and polyaxonal cells in four (Fig. 5G,K,M,N).

Synaptic mechanisms

The next series of experiments investigated the mechanisms through which ipRGCs transmit photoresponses to displaced amacrine cells. Based on a previous report of tracer coupling [10], we hypothesized that our sustained amacrines received ipRGC input through electrical synapses. To test this, we isolated melanopsin-driven light responses using the glutamate blockers, and added 50 – 100 μM meclofenamic acid (MFA) to block gap junctions [15]. All amacrine cells' (n = 11) melanopsin-mediated light responses were dramatically reduced, indicating a critical role for gap junctions (Fig. 6A).

Many amacrine cells signal to each other through glycine and GABA [16]. Thus, ipRGCs could conceivably transmit excitatory photoresponses not only to directly coupled amacrine cells, but also to amacrine cells receiving polysynaptic disinhibitory input from ipRGC-coupled amacrines. To test this possibility, we blocked $GABA_A$, $GABA_B$, $GABA_C$ and glycine receptors using 10 μM bicuculline, 20 μM CGP52432 (3-[[(3,4-dichlorophenyl)methyl]amino]propyl(diethoxymethyl)phosphinic acid), 20 μM TPMPA ((1,2,5,6-tetrahydropyridin-4-yl)methylphosphinic acid) and 10 μM strychnine, respectively. For all cells tested (n = 7), melanopsin-driven light responses were intact if not enhanced (Fig. 6B), suggesting GABAergic/glycinergic disinhibition is probably not involved in transmitting ipRGC signals.

In all the experiments presented so far, rod/cone-driven light responses were blocked using L-AP4, DNQX and D-AP5, which completely disrupt signaling from the outer retina to the inner retina. However, DNQX and D-AP5 also antagonize ionotropic glutamatergic transmission within the IPL. Thus, if ipRGCs signal to some displaced amacrine cells through ionotropic glutamate receptors, using these three drugs to find rod/cone-independent photoresponses would have caused us to miss such amacrines. To test this possibility, we spent six weeks searching for spiking sustained ON displaced amacrines in the presence of L-AP4, which abolishes ON bipolar cells' photosensitivity while sparing ionotropic glutamatergic transmission [17]. Twelve such cells were encountered, and all their light responses were minimally affected by the addition of DNQX and D-AP5 (Fig. 6C). In conclusion, ionotropic glutamate receptors do not mediate ipRGC signaling to displaced amacrine cells.

ipRGC transmission to DA cells can be blocked by the voltage-gated Na^+ channel antagonist tetrodotoxin (TTX) [18]. We next tested whether this applies also to ipRGC-driven displaced amacrine cells. While 600 nM TTX eliminated all spiking activity in these neurons, the graded component of their melanopsin-driven photoresponses was largely intact (Fig. 6D), indicating voltage-gated Na^+ channels are not required for signal transmission from ipRGCs. However, these graded light responses were significantly reduced (p = 0.0016), implying an involvement of these channels.

The rod/cone input is also sustained

Although melanopsin is well-known for its ability to evoke tonic light responses [5, 13] (see also Figs. 2C and 3B), rod/cone-driven networks can also support remarkably long-lasting inner retinal photoresponses [8]. We next tested whether rod/cone input is sufficient to evoke sustained photoresponses in ipRGC-driven displaced amacrine cells. Light responses were recorded from them first in normal Ames', and again after adding 50 – 100 μM MFA to block gap junctions including those connecting ipRGCs to amacrine cells. In the presence of MFA, these amacrine cells' photoresponses ended abruptly at light offset, suggesting effective block of ipRGC input (Fig. 7A,B). MFA made the light responses somewhat more transient, with a steady state that was more hyperpolarized than that observed before MFA treatment (Fig. 7A,B), and the final-to-peak amplitude ratio was reduced from 0.52±0.04 to 0.37±0.06 (p = 0.016) (Fig. 7C). But these responses remained depolarized throughout the 10-s light, with an accompanying sustained elevation in spiking (Fig. 7A). In conclusion,

rod/cone input can drive sustained photoresponses in these cells, though adding ipRGC input makes them even more tonic. This suggests that the light responses of ipRGCs should be more sustained than those of the ipRGC-coupled amacrines, and indeed, the final-to-peak amplitude ratio for the former (Fig. 7D) was significantly higher ($p < 0.001$) than for the latter (Fig. 7C *left column*).

DISCUSSION

Light responses of rare amacrine cells and origins of sustained signals

Due to their low abundance, most wide-field amacrine cells have been little studied. In salamander, amacrine cells include wide- *vs.* narrow-field varieties, which generate transient and sustained light responses respectively [19]. By contrast, in mammalian retinas, both transient [20–23] and sustained responses [24] have been recorded from wide-field amacrine cells, and also from narrow-field ones [25]. Here, we detected spiking, sustained ON light responses in displaced rat amacrine cells with very diverse field sizes. If we categorize cells with 200 – 500 μm fields as medium-field and larger ones as wide-field [26], ~80% of our cells were wide-field. Thus, at least in the GCL, most spiking sustained ON amacrines are wide-field, the opposite of that observed for salamander.

Zhang and colleagues reported that among mouse DA cells, those with ipRGC input displayed tonic light responses while the rest had transient responses, suggesting DA cells might require melanopsin input to generate sustained responses [5]. Although we likewise found all spiking sustained ON displaced amacrines to be ipRGC-driven, melanopsin cannot be the sole source of tonic information since they were still tonic when ipRGC input was blocked by MFA. This result has one caveat, however, because MFA disrupted not only ipRGC-amacrine coupling, but also gap junctions throughout the retina, which could have made normally transient rod/cone circuits more sustained. Nevertheless, we previously learned that even with melanopsin knocked out, long-lasting inner retinal photoresponses were still readily detectable [8]. Moreover, many non-spiking amacrine cells have sustained, non-ipRGC-mediated responses (Fig. 1). An obvious question is, if the rod/cone input is sufficient to drive tonic responses, why would the spiking sustained ON amacrines also need ipRGC input? A plausible reason is that their functional roles require them to generate photoresponses even more tonic than can be supported by the rod/cone input. By drawing input from ipRGCs as well as rod/cone circuits, these amacrine cells ensure that their light responses are sufficiently tonic.

Synaptic circuits mediating ipRGC signaling to displaced amacrine cells

Coupling between amacrine cells and RGCs has been proposed to allow the former to regulate the latter, e.g. increasing receptive field size and contrast sensitivity [27], synchronizing RGCs' firing activities and enhancing their motion sensitivity [28], and providing an excitatory input to RGCs [29]. Here, we report electrical signaling in the opposite direction, allowing ipRGCs to propagate their tonic photoresponses to amacrine cells. Both mouse and rat possess five types of ipRGCs (M1 – M5) with different light responses [11, 30]. Using mice containing fluorescently labeled M1 – M3 ipRGCs, Müller *et al.* found tracer coupling between these three types and displaced amacrine cells [10]. The

alpha-like M4 type is probably also connected to displaced amacrines because ON alpha cells are well-known to be amacrine-coupled [31, 32]. Thus, our ipRGC-coupled amacrines could be driven by any of these four types, and the three morphological classes' photoresponse diversity raises the possibility that they draw input from different ipRGCs. Notably, the bistratifying amacrine cells' melanopsin-mediated responses usually peaked faster than those of the other morphological groups (Fig. 5G,N), suggesting they might be coupled to M1 cells, which have the fastest intrinsic light responses among ipRGCs [11]. Reinforcing this possibility, these bistratified cells are the only ipRGC-coupled amacrines to have dendrites in the S1 sublamina, where they could contact M1 cells' S1-stratifying dendrites.

ipRGC-amacrine coupling was first proposed by Sekaran *et al.*, who observed that the gap junction blocker carbenoxolone abolished the light-evoked Ca^{2+} dye responses in about half of all photosensitive GCL somas in rodless coneless retinas [33]. This conclusion became questionable when subsequent work showed that the percentage of light-responsive GCL neurons detected by Sekaran *et al.* (~3%) roughly matched the percentage of ipRGCs [34], and that carbenoxolone could block the light-induced Ca^{2+} dye responses of dissociated ipRGCs [35]. However, the demonstration of tracer coupling strengthened the possibility of ipRGC-amacrine coupling [10], which we validated here.

Some ipRGCs' axons extend collaterals [36], which have been proposed to innervate the sustained DA cells [18]. These glutamatergic collaterals are unlikely to contact our displaced amacrine cells, because robust melanopsin-driven light responses persisted in the presence of DNQX and D-AP5. The fact that ipRGC signaling to displaced amacrines survived the glutamate blockers further ruled out any requirement for cholinergic or dopaminergic transmission, because glutamate block abolishes the photoresponses of cholinergic starburst cells (Fig. 1; ref. [37]) and DA cells [5, 38]. Disinhibitory GABAergic/glycinergic synapses probably also do not participate in signaling from ipRGC-coupled amacrine cells to other amacrines, as melanopsin-driven light responses were not weakened by GABA/glycine antagonists. Thus, gap junctions mediate all synaptic transmission from ipRGCs to displaced amacrine cells.

Displaced amacrine cells' melanopsin-driven light responses survived TTX, suggesting signaling from ipRGCs does not require Na^+ spikes. TTX did reduce these responses, however, indicating ipRGC signaling is facilitated by voltage-gated Na^+ channels, and indeed wide-field amacrines often use active conductances to boost long-range propagation [21, 39, 40]. Such partial reliance on voltage gating suggests that ipRGCs' light responses might travel fairly far to reach the coupled amacrine cells. This may be especially true for the medium-field amacrine cells because RGCs are directly coupled only to wide-field and polyaxonal amacrines [41], so these medium-field cells presumably connect electrically to ipRGCs by way of wide-field and/or polyaxonal cells.

The extent of intraretinal signaling by ipRGCs

Half of all rat GCL neurons are displaced amacrines [42]. Thus, assuming we sampled randomly from all soma sizes, half of the recorded cells (~1,950) were amacrine cells, and the 154 ipRGC-driven amacrines constituted 7.9% of this population. In mouse, ~11% of

displaced amacrine cells are RGC-coupled [29]. If that percentage also applies to rat, then ~70% of RGC-coupled displaced amacrine cells are connected to ipRGCs, although this is likely an overestimate since ref. [29] focused on cells directly coupled to RGCs, whereas some of our amacrines could have been coupled to ipRGCs indirectly.

Although conservative morphological criteria grouped our ipRGC-driven amacrines into only three categories, the wide range of field sizes suggests that each category probably comprised multiple cell types. Following Müller and colleagues' nomenclature for displaced amacrines and their use of 500 μm as the cutoff between medium and wide fields [26], our ipRGC-driven cells included five types: MA-S5, MA-S1/S5, WA-S5, WA-S1/S5, and PA-S5. While Müller *et al.* did not encounter WA-S5 or WA-S1/S5 in mouse, both have been seen in rat [43]. The >30 morphological types of amacrine cells secrete various neuromodulators, which diffuse to other retinal neurons to regulate their physiology [44, 45]. Finding out what neuromodulators are used by the ipRGC-coupled amacrine cells would provide insights into how these neurons might influence retinal physiology. At least eleven neuromodulators have been detected in displaced rat amacrine cells: cholecystokinin [46], corticotropin releasing factor [47], dopamine [14], epinephrine [48], neurokinin A and B [49], neuropeptide Y [50], nitric oxide [51], somatostatin [52], substance P [53], and vasoactive intestinal peptide [54]. We have shown that ipRGC-coupled rat amacrine cells are not dopaminergic (Fig. 4G), and preliminary experiments have further ruled out neuropeptide Y and somatostatin (data not shown).

There are likely even more ipRGC-driven amacrine cells in the inner nuclear layer (INL). Using the immediate early gene *c-fos* to label light-activated neurons in mice lacking rod/cone function, Barnard and colleagues showed that light excited four-fold more cells in the INL than in the GCL [55]. Since the INL contains only a few displaced ipRGCs [56], the vast majority of the FOS-positive INL cells were presumably ipRGC-driven amacrines, which far outnumbered the FOS-stained ipRGCs and ipRGC-coupled amacrines in the GCL.

EXPERIMENTAL PROCEDURES

Whole-cell recording

Methods for euthanasia, eyecup generation, whole-cell recording and photostimulation were described in detail previously [11]. Briefly, eyecups were harvested from dark-adapted Sprague Dawley rats and cut into quadrants. One quadrant was flattened on a superfusion chamber, superfused with 32 °C Ames' medium, and kept in darkness except during light presentation. The GCL was visualized through infrared transillumination and whole-cell recording obtained from randomly selected somas using an internal solution containing (in mM) 120 K-gluconate; 9 Neurobiotin-Cl; 10 Hepes; 2 EGTA; 4 Mg-ATP; 0.3 Na-GTP; 7 Tris-phosphocreatine; 0.1% Lucifer Yellow; and KOH to set pH at 7.3. All stimuli were full-field 480-nm light, with intensity adjusted using neutral density filters. Pairwise statistical comparisons were made using the Student's *t*-test, with $p < 0.05$ indicating significant differences. All error values are S.E.M.

In the experiment measuring light responses in retinally degenerate mice, we used CBA/J mice carrying the *Pde6b*^{rd1} mutation (Jackson Laboratory 000656; Bar Harbor, ME) that

were at least 9 months old. Experimental procedures were identical to the above, except that isolated retinas were used.

Morphological characterization

The methods for immunohistochemistry and morphological analysis have also been detailed previously [11]. Briefly, each recorded retina was fixed in 4% paraformaldehyde for 12 – 20 min and incubated in one or more of the following primary antibodies: goat-anti-ChAT (EMD Millipore AB144P, 1:200; Billerica, MA), mouse-anti-GABA (Sigma A0310, 1:100; St. Louis, MO), rabbit-anti-RBPMS (PhosphoSolutions 1830-RBPMS, 1:300; Aurora, CO), rabbit-anti-tyrosine hydroxylase (EMD Millipore AB152, 1:200), and rabbit anti-Lucifer Yellow (Life Technologies A-5750, 1:500; Grand Island, NY). These antibodies were visualized through staining with the following secondary antibodies, all raised in donkey: anti-goat Cy3 (Jackson ImmunoResearch 705-165-147; 1:250; West Grove, PA), anti-goat Cy5 (Jackson ImmunoResearch 705-175-147; 1:250), anti-mouse DyLight 405 (Jackson ImmunoResearch 715-475-151; 1:60), anti-rabbit FITC (Jackson ImmunoResearch 711-095-152; 1:200), and anti-rabbit Cy3 (Jackson ImmunoResearch 711-165-152; 1:200). To visualize Neurobiotin fills, Alexa-conjugated streptavidin (Life Technologies, 1:700; Grand Island, NY) was included during both primary and secondary antibody incubation.

Recorded cells were imaged through confocal microscopy at 0.38-μm z-steps, and dendritic stratification levels determined in rotated images. The “equivalent circle” method was used to quantify a cell’s field size: after drawing straight lines to connect the tips of all processes in the confocal z-projection, we measured the resultant polygon’s area and expressed field diameter as the diameter of the circle whose area matched the polygon’s. In the figures showing the streptavidin or Lucifer Yellow staining of recorded cells, all extracellular staining was masked manually.

ACKNOWLEDGEMENTS

This work was funded by National Eye Institute (NEI) grants R00 EY018863 and R01 EY023660 to K.Y.W., a Research to Prevent Blindness Scientific Career Development Award to K.Y.W., a Health Sciences Scholars Program Summer Research Stipend to B.Y.L., and NEI Vision Core Grant P30 EY007003 to the Kellogg Eye Center.

REFERENCES

1. Masland RH. The fundamental plan of the retina. Nat Neurosci. 2001; 4:877–886. [PubMed: 11528418]
2. Dong CJ, Werblin FS. Temporal contrast enhancement via GABAC feedback at bipolar terminals in the tiger salamander retina. J Neurophysiol. 1998; 79:2171–2180. [PubMed: 9535976]
3. Dixon DB, Copenhagen DR. Two types of glutamate receptors differentially excite amacrine cells in the tiger salamander retina. J Physiol. 1992; 449:589–606. [PubMed: 1355793]
4. Maguire G. Rapid desensitization converts prolonged glutamate release into a transient EPSC at ribbon synapses between retinal bipolar and amacrine cells. Eur J Neurosci. 1999; 11:353–362. [PubMed: 9987038]
5. Zhang DQ, Wong KY, Sollars PJ, Berson DM, Pickard GE, McMahon DG. Intraretinal signaling by ganglion cell photoreceptors to dopaminergic amacrine neurons. Proc Natl Acad Sci U S A. 2008; 105:14181–14186. [PubMed: 18779590]

6. Brown TM, Tsujimura S, Allen AE, Wynne J, Bedford R, Vickery G, Vugler A, Lucas RJ. Melanopsin-based brightness discrimination in mice and humans. Current biology : CB. 2012; 22:1134–1141. [PubMed: 22633808]
7. Guler AD, Ecker JL, Lall GS, Haq S, Altimus CM, Liao HW, Barnard AR, Cahill H, Badea TC, Zhao H, et al. Melanopsin cells are the principal conduits for rod-cone input to non-image-forming vision. Nature. 2008; 453:102–105. [PubMed: 18432195]
8. Wong KY. A retinal ganglion cell that can signal irradiance continuously for 10 hours. J Neurosci. 2012; 32:11478–11485. [PubMed: 22895730]
9. Dkhissi-Benyahya O, Coutanson C, Knoblauch K, Lahouaoui H, Leviel V, Rey C, Bennis M, Cooper HM. The absence of melanopsin alters retinal clock function and dopamine regulation by light. Cell Mol Life Sci. 2013; 70:3435–3447. [PubMed: 23604021]
10. Muller LP, Do MT, Yau KW, He S, Baldridge WH. Tracer coupling of intrinsically photosensitive retinal ganglion cells to amacrine cells in the mouse retina. J Comp Neurol. 2010; 518:4813–4824. [PubMed: 20963830]
11. Reifler AN, Chervenak AP, Dolikian ME, Benenati BA, Meyers BS, Demertzis ZD, Lynch AM, Li BY, Wachter RD, Abufarha FS, et al. The rat retina has five types of ganglion-cell photoreceptors. Exp Eye Res. 2015; 130:17–28. [PubMed: 25450063]
12. Rodriguez AR, de Sevilla Muller LP, Brecha NC. The RNA binding protein RBPMS is a selective marker of ganglion cells in the mammalian retina. J Comp Neurol. 2014; 522:1411–1443. [PubMed: 24318667]
13. Berson DM, Dunn FA, Takao M. Phototransduction by retinal ganglion cells that set the circadian clock. Science. 2002; 295:1070–1073. [PubMed: 11834835]
14. Martin-Martinelli E, Savy C, Nguyen-Legros J. Morphometry and distribution of displaced dopaminergic cells in rat retina. Brain research bulletin. 1994; 34:467–482. [PubMed: 8082039]
15. Pan F, Mills SL, Massey SC. Screening of gap junction antagonists on dye coupling in the rabbit retina. Vis Neurosci. 2007; 24:609–618. [PubMed: 17711600]
16. Chen X, Hsueh HA, Werblin FS. Amacrine-to-amacrine cell inhibition: Spatiotemporal properties of GABA and glycine pathways. Vis Neurosci. 2011; 28:193–204. [PubMed: 21676336]
17. Slaughter MM, Miller RF. 2-amino-4-phosphonobutyric acid: a new pharmacological tool for retina research. Science. 1981; 211:182–185. [PubMed: 6255566]
18. Atkinson, C.; Zhang, D. Association for Research in Vision and Ophthalmology. Orlando, FL: 2014. Action potential-dependent calcium influx into ganglion cell photoreceptors mediates retrograde signal transmission to dopaminergic amacrine neurons.
19. Werblin F, Maguire G, Lukasiewicz P, Eliasof S, Wu SM. Neural interactions mediating the detection of motion in the retina of the tiger salamander. Vis Neurosci. 1988; 1:317–329. [PubMed: 2856477]
20. Taylor WR. Response properties of long-range axon-bearing amacrine cells in the dark-adapted rabbit retina. Vis Neurosci. 1996; 13:599–604. [PubMed: 8870218]
21. Bloomfield SA, Volgyi B. Response properties of a unique subtype of wide-field amacrine cell in the rabbit retina. Vis Neurosci. 2007; 24:459–469. [PubMed: 17900375]
22. Dacheux RF, Raviola E. Light responses from one type of ON-OFF amacrine cells in the rabbit retina. J Neurophysiol. 1995; 74:2460–2468. [PubMed: 8747206]
23. Knop GC, Pottek M, Monyer H, Weiler R, Dedek K. Morphological and physiological properties of enhanced green fluorescent protein (EGFP)-expressing wide-field amacrine cells in the ChAT-EGFP mouse line. Eur J Neurosci. 2014; 39:800–810. [PubMed: 24299612]
24. Nelson R, Kolb H. A17: a broad-field amacrine cell in the rod system of the cat retina. J Neurophysiol. 1985; 54:592–614. [PubMed: 4045539]
25. Pang JJ, Gao F, Wu SM. Physiological characterization and functional heterogeneity of narrow-field mammalian amacrine cells. J Physiol. 2012; 590:223–234. [PubMed: 22083601]
26. Perez De Sevilla Muller L, Shelley J, Weiler R. Displaced amacrine cells of the mouse retina. J Comp Neurol. 2007; 505:177–189. [PubMed: 17853452]
27. Dacey DM, Brace S. A coupled network for parasol but not midget ganglion cells in the primate retina. Vis Neurosci. 1992; 9:279–290. [PubMed: 1390387]

28. Kenyon GT, Marshak DW. Gap junctions with amacrine cells provide a feedback pathway for ganglion cells within the retina. Proc Biol Sci. 1998; 265:919–925. [PubMed: 9633113]
29. Pang JJ, Paul DL, Wu SM. Survey on amacrine cells coupling to retrograde-identified ganglion cells in the mouse retina. Invest Ophthalmol Vis Sci. 2013; 54:5151–5162. [PubMed: 23821205]
30. Zhao X, Stafford BK, Godin AL, King WM, Wong KY. Photoresponse diversity among the five types of intrinsically photosensitive retinal ganglion cells. J Physiol. 2014; 592:1619–1636. [PubMed: 24396062]
31. Schubert T, Degen J, Willecke K, Hormuzdi SG, Monyer H, Weiler R. Connexin36 mediates gap junctional coupling of alpha-ganglion cells in mouse retina. J Comp Neurol. 2005; 485:191–201. [PubMed: 15791644]
32. Volgyi B, Abrams J, Paul DL, Bloomfield SA. Morphology and tracer coupling pattern of alpha ganglion cells in the mouse retina. J Comp Neurol. 2005; 492:66–77. [PubMed: 16175559]
33. Sekaran S, Foster RG, Lucas RJ, Hankins MW. Calcium imaging reveals a network of intrinsically light-sensitive inner-retinal neurons. Current biology : CB. 2003; 13:1290–1298. [PubMed: 12906788]
34. Ecker JL, Dumitrescu ON, Wong KY, Alam NM, Chen SK, LeGates T, Renna JM, Prusky GT, Berson DM, Hattar S. Melanopsin-expressing retinal ganglion-cell photoreceptors: cellular diversity and role in pattern vision. Neuron. 2010; 67:49–60. [PubMed: 20624591]
35. Bramley JR, Wiles EM, Sollars PJ, Pickard GE. Carbenoxolone blocks the light-evoked rise in intracellular calcium in isolated melanopsin ganglion cell photoreceptors. PLoS One. 2011; 6:e22721. [PubMed: 21829491]
36. Joo HR, Peterson BB, Dacey DM, Hattar S, Chen SK. Recurrent axon collaterals of intrinsically photosensitive retinal ganglion cells. Vis Neurosci. 2013; 30:175–182. [PubMed: 23834959]
37. Taylor WR, Wassle H. Receptive field properties of starburst cholinergic amacrine cells in the rabbit retina. Eur J Neurosci. 1995; 7:2308–2321. [PubMed: 8563980]
38. Zhang DQ, Zhou TR, McMahon DG. Functional heterogeneity of retinal dopaminergic neurons underlying their multiple roles in vision. J Neurosci. 2007; 27:692–699. [PubMed: 17234601]
39. Heflin SJ, Cook PB. Narrow and wide field amacrine cells fire action potentials in response to depolarization and light stimulation. Vis Neurosci. 2007; 24:197–206. [PubMed: 17640411]
40. Cook PB, Werblin FS. Spike initiation and propagation in wide field transient amacrine cells of the salamander retina. J Neurosci. 1994; 14:3852–3861. [PubMed: 7911519]
41. Volgyi B, Chheda S, Bloomfield SA. Tracer coupling patterns of the ganglion cell subtypes in the mouse retina. J Comp Neurol. 2009; 512:664–687. [PubMed: 19051243]
42. Schlamp CL, Montgomery AD, Mac Nair CE, Schuart C, Willmer DJ, Nickells RW. Evaluation of the percentage of ganglion cells in the ganglion cell layer of the rodent retina. Mol Vis. 2013; 19:1387–1396. [PubMed: 23825918]
43. Perry VH, Walker M. Amacrine cells, displaced amacrine cells and interplexiform cells in the retina of the rat. Proc R Soc Lond B Biol Sci. 1980; 208:415–431. [PubMed: 6158054]
44. Brecha, NC. Peptide and peptide receptor expression and function in the vertebrate retina. In: Chalupa, LM.; Werner, JS., editors. The Visual Neurosciences. Vol. 1. Cambridge, MA: MIT Press; 2004. p. 334-354.
45. Dowling, JE. The retina: an approachable part of the brain. revised edition. Cambridge, MA: The Belknap Press of Harvard University Press; 2012. Edition
46. Firth SI, Varela C, De la Villa P, Marshak DW. Cholecystokinin-like immunoreactive amacrine cells in the rat retina. Vis Neurosci. 2002; 19:531–540. [PubMed: 12511085]
47. Yeh HH, Olschowka JA. A system of corticotropin releasing factor-containing amacrine cells in the rat retina. Neuroscience. 1989; 33:229–240. [PubMed: 2601858]
48. Hadjiconstantinou M, Mariani AP, Panula P, Joh TH, Neff NH. Immunohistochemical evidence for epinephrine-containing retinal amacrine cells. Neuroscience. 1984; 13:547–551. [PubMed: 6392928]
49. Brecha NC, Sternini C, Anderson K, Krause JE. Expression and cellular localization of substance P/neurokinin A and neurokinin B mRNAs in the rat retina. Vis Neurosci. 1989; 3:527–535. [PubMed: 2484823]

50. Oh SJ, D'Angelo I, Lee EJ, Chun MH, Brecha NC. Distribution and synaptic connectivity of neuropeptide Y-immunoreactive amacrine cells in the rat retina. J Comp Neurol. 2002; 446:219–234. [PubMed: 11932938]

51. Chun MH, Oh SJ, Kim IB, Kim KY. Light and electron microscopical analysis of nitric oxide synthase-like immunoreactive neurons in the rat retina. Vis Neurosci. 1999; 16:379–389. [PubMed: 10367971]

52. Larsen JN, Bersani M, Olcese J, Holst JJ, Moller M. Somatostatin and prosomatostatin in the retina of the rat: an immunohistochemical, in-situ hybridization, and chromatographic study. Vis Neurosci. 1990; 5:441–452. [PubMed: 1981146]

53. Zhang D, Yeh HH. Substance-P-like immunoreactive amacrine cells in the adult and the developing rat retina. Brain Res Dev Brain Res. 1992; 68:55–65. [PubMed: 1381664]

54. Casini G, Molnar M, Brecha NC. Vasoactive intestinal polypeptide/peptide histidine isoleucine messenger RNA in the rat retina: adult distribution and developmental expression. Neuroscience. 1994; 58:657–667. [PubMed: 8170541]

55. Barnard AR, Appleford JM, Sekaran S, Chinthapalli K, Jenkins A, Seeliger M, Biel M, Humphries P, Douglas RH, Wenzel A, et al. Residual photosensitivity in mice lacking both rod opsin and cone photoreceptor cyclic nucleotide gated channel 3 alpha subunit. Vis Neurosci. 2004; 21:675–683. [PubMed: 15683556]

56. Hattar S, Liao HW, Takao M, Berson DM, Yau KW. Melanopsin-containing retinal ganglion cells: architecture, projections, and intrinsic photosensitivity. Science. 2002; 295:1065–1070. [PubMed: 11834834]

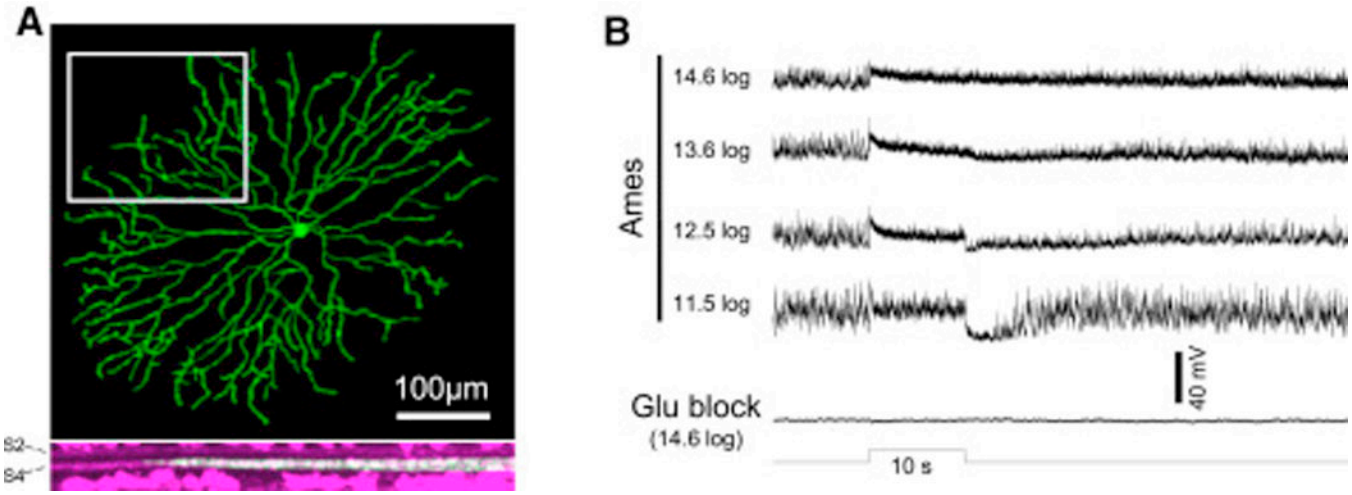

Figure 1. Non-spiking, sustained ON amacrine cells lost photosensitivity during rod/cone signaling block

A) The Lucifer Yellow fill of one such neuron, which was a starburst cell. *Top*: Confocal z-projection. *Bottom*: The rotated view of the region highlighted by the rectangle in the *top panel*. The magenta staining represents ChAT labeling, which marks S2 and S4 of the IPL. *B)* Light responses from another non-spiking sustained amacrine cell, recorded during superfusion by normal Ames' medium (*top recordings*) and after the addition of 50 µM L-AP4, 40 µM DNQX and 25 µM D-AP5 ("glutamate blockers") to disrupt rod/cone signaling (*bottom recording*). The log values indicate light intensity in photons cm^{-2} s^{-1}.

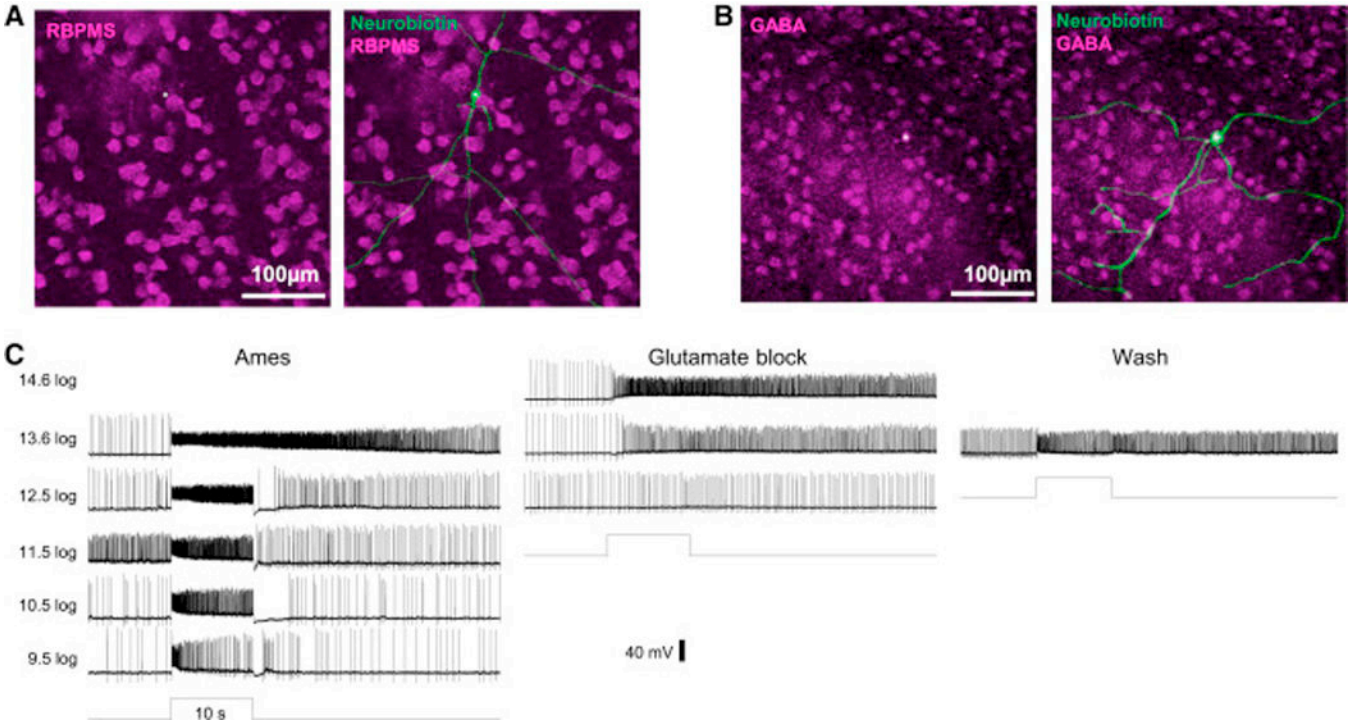

Figure 2. All spiking, sustained ON displaced amacrine cells remained light-sensitive during rod/cone signaling block

A) Besides their lack of ganglion-cell axons, these sustained ON cells' identity as amacrine cells was confirmed by their lack of the RGC marker RBPMS (*magenta*). *B)* Most sustained ON amacrine cells tested for GABA immunostaining were stained (*magenta*). In both *A* and *B*, Neurobiotin in the recorded cells was visualized by Alexa488- conjugated streptavidin (*green*), and their somas are indicated by asterisks. *C)* Typical light responses from a spiking sustained ON displaced amacrine cell, recorded in normal Ames' (*left recordings*), in the presence of glutamate blockers (*middle recordings*), and after washout of the drugs (*right recording*).

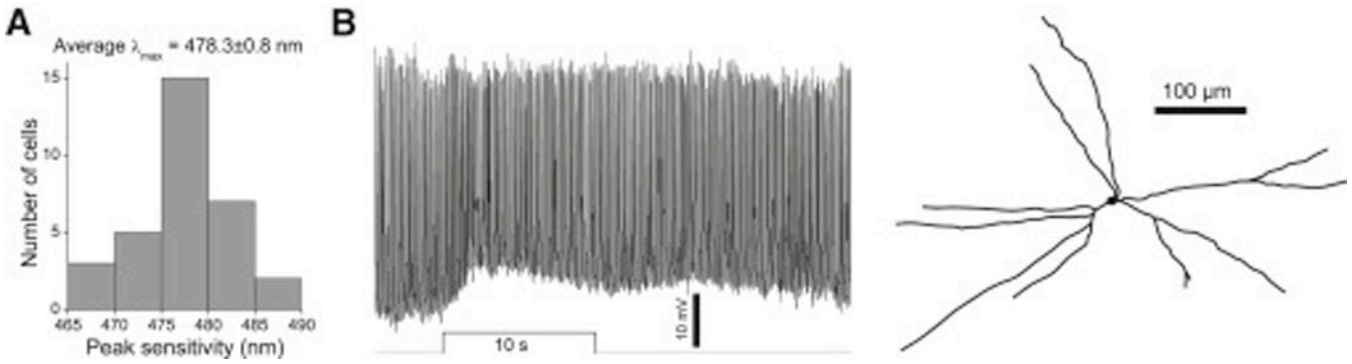

Figure 3. Spiking, sustained ON displaced amacrine cells receive ipRGC input

A) λ_{max} for the light responses of 32 sustained ON displaced amacrines measured in the presence of glutamate blockers. The mean λ_{max} was close to that for melanopsin. *B)* The light response and morphology of a photosensitive displaced amacrine cell from a retinally degenerate mouse. All dendrites of this cell stratified in S5 of the IPL. Light intensity was 15.3 log photons cm^{-2} s^{-1}.

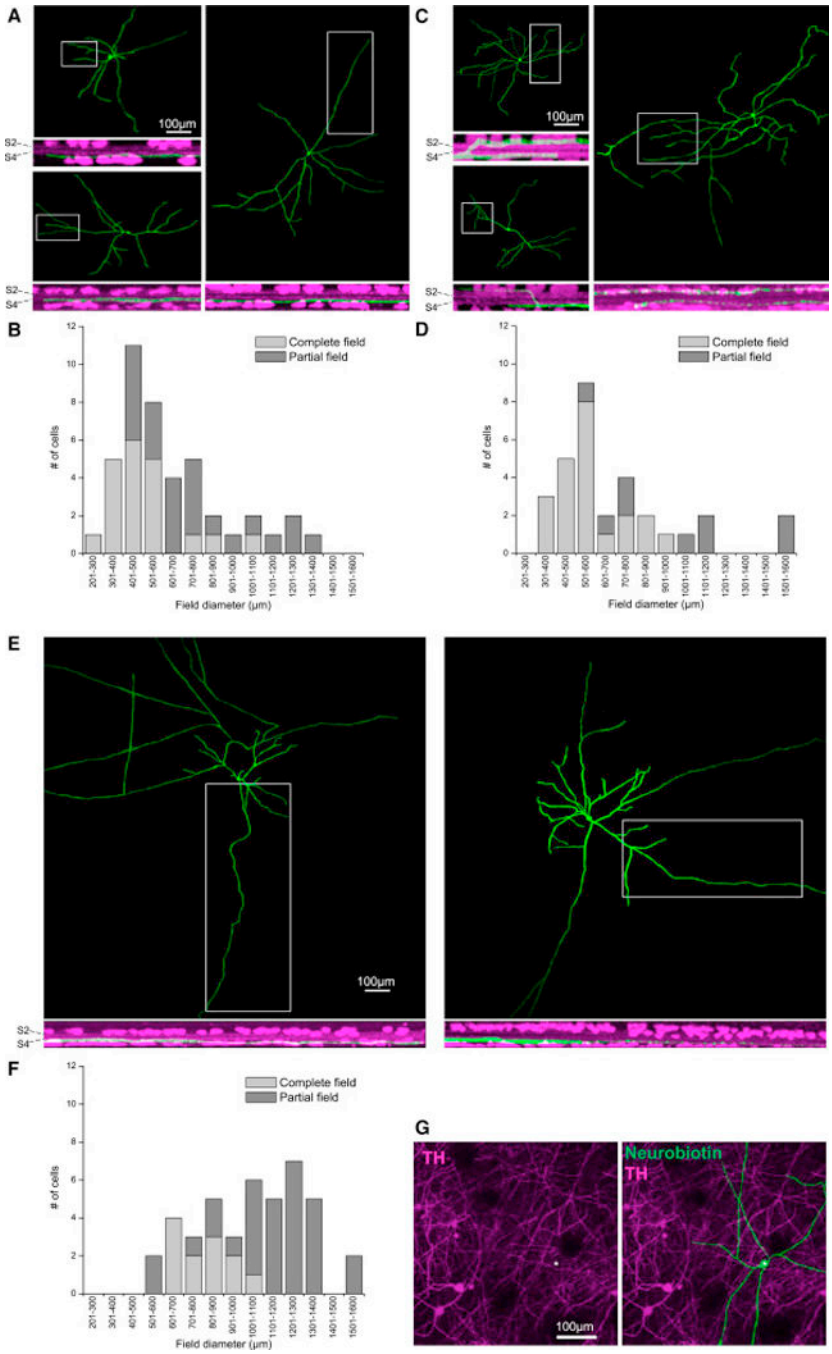

Figure 4. Morphologies of ipRGC-driven displaced amacrine cells

A – F) Confocal images and field size distributions of spiking, sustained ON displaced amacrines monostratifying in S5 of the IPL (*A*,*B*), those bistratifying in S1 and S5 (*C*,*D*), and polyaxonal cells (*E*,*F*). For the field diameter measurements (*B*, *D* and *F*), we used not only cells whose entire fields were imaged (*light columns*), but also those with incompletely imaged fields (*dark columns*). *G)* ipRGC-driven displaced amacrines are not dopaminergic. Dopaminergic amacrine cells were identified by antibody staining against tyrosine hydroxylase (TH), and the somas of four TH+ cells in the inner nuclear layer are within the

field of view. The Neurobiotin-filled ipRGC-driven displaced amacrine cell (*asterisk*) lacked TH immunostaining.

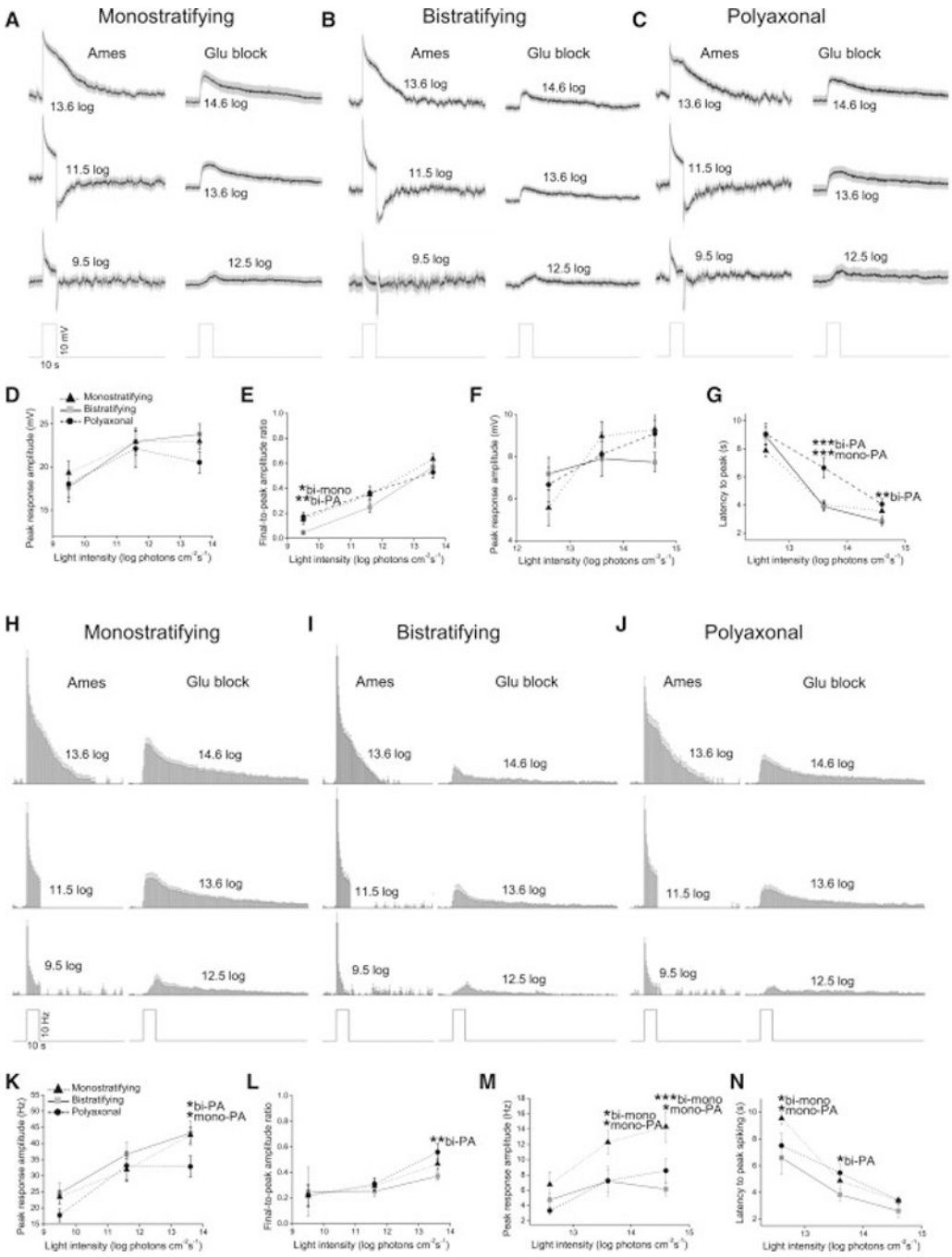

Figure 5. Light responses of ipRGC-driven displaced amacrine cells

The light responses of 21 monostratifying cells, 15 bistratifying cells and 21 polyaxonal cells were averaged and quantified. Graded responses are shown in *A – G* and spiking responses in *H – N*. *A – C)* The averaged graded light responses, recorded in the presence of normal Ames' medium (*left traces*) and glutamate blockers (*right traces*). Spikes were removed by 10 Hz low-pass filtering. The gray areas around the averaged traces represent S.E.M. *D,E)* Peak amplitude and final-topeak amplitude ratio of the light responses recorded in normal Ames'. *F,G)* Peak amplitude and latency of the light responses recorded during

glutamate block. *H – J)* Averaged histograms of spiking photoresponses, recorded during normal Ames' superfusion (*left histograms*) and glutamate block (*right histograms*). *K,L)* Peak amplitude and final-to-peak amplitude ratio of the spiking responses recorded in normal Ames'. *M,N)* Peak amplitude and latency of the spiking responses during glutamate block. All error bars are S.E.M. *, $p < 0.05$; **, $p < 0.01$; ***, $p < 0.001$.

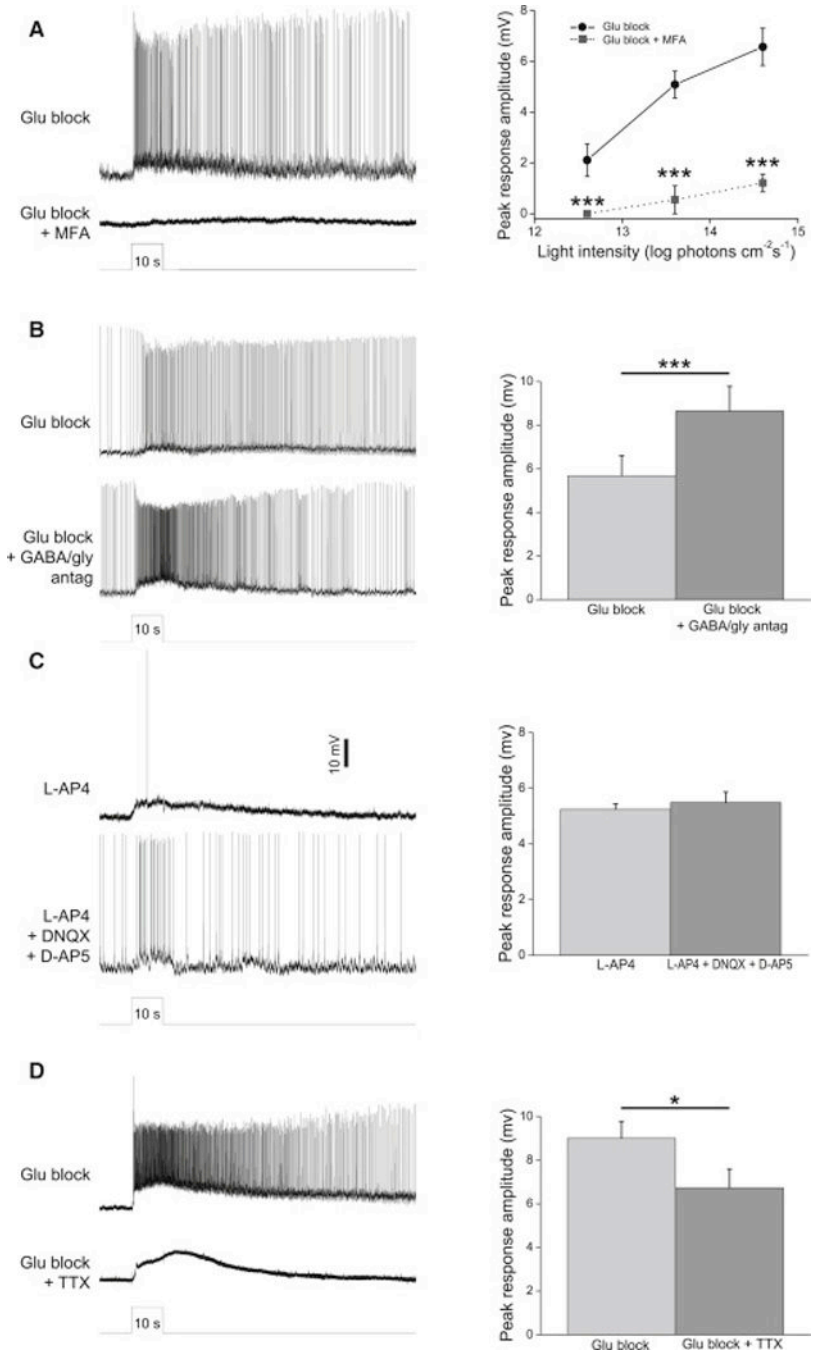

Figure 6. Synaptic mechanisms for ipRGC signaling to displaced amacrine cells

A) The gap junction blocker MFA (50 – 100 μM) nearly abolished the melanopsin-driven light responses of spiking sustained ON displaced amacrines. *Left*, example recordings from a polyaxonal cell. Light intensity was 13.6 log photons cm^{-2} s^{-1}. *Right*, population data from all 11 cells tested (3 monostratified, 5 bistratified, 3 polyaxonal). *B)* Melanopsin-driven light responses were not reduced by a cocktail containing $GABA_A$, $GABA_B$, $GABA_C$ and glycine receptor antagonists. *Left*, example recordings from a monostratified cell. *Right*, population data from all 10 cells tested (5 monostratified, 4 bistratified, 1 polyaxonal). *C)*

All cells that gave spiking sustained ON light responses in the presence of L-AP4 remained photosensitive after the addition of DNQX and DAP5. *Left*, example recordings from a bistratified cell. *Right*, population data from all 10 cells tested (3 monostratified, 4 bistratified, 3 polyaxonal). *D)* The voltage-gated Na^+ channel blocker TTX (600 nM) did not abolish displaced amacrine cells' melanopsin-driven light responses, though it eliminated all spikes. *Left*, example recordings from a polyaxonal cell. *Right*, population data from all 11 cells tested (6 monostratified, 1 bistratified, 4 polyaxonal). Light intensity was 13.6 log photons cm^{-2} s^{-1} in *B* through *D*. *, $p < 0.05$; ***, $p < 0.001$.

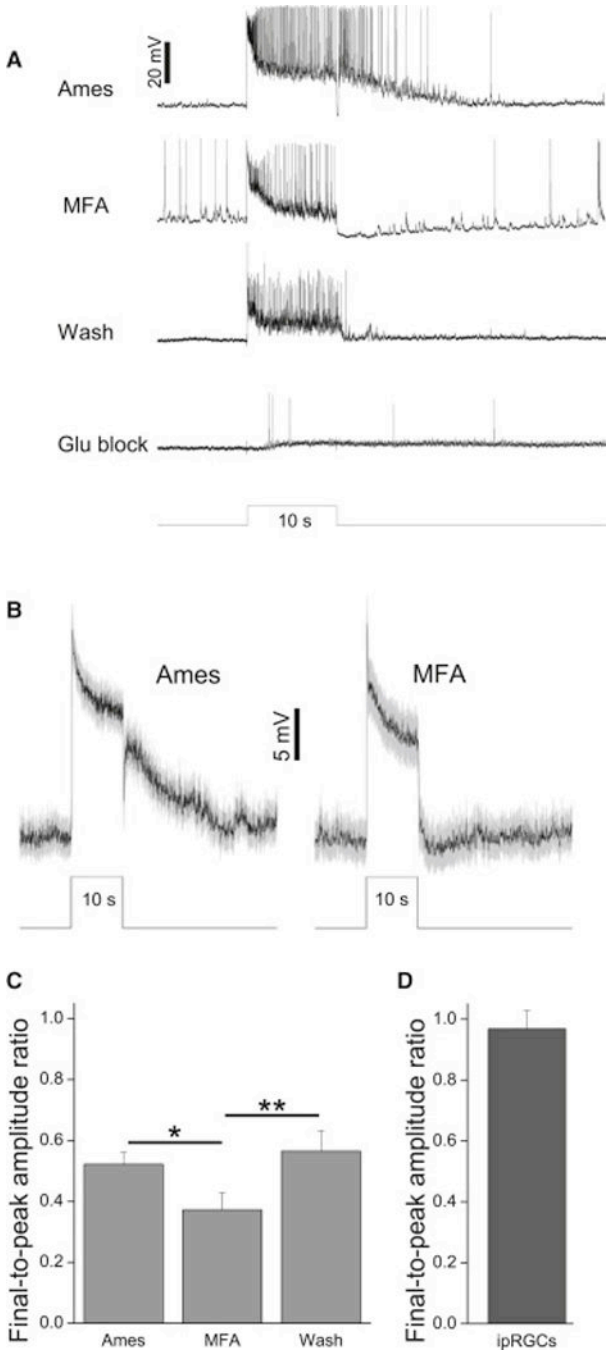

Figure 7. Rod/cone input to ipRGC-driven displaced amacrine cells is tonic

A) A monostratified amacrine cell's light responses remained sustained during disruption of ipRGC input by MFA. At the end of this experiment, this cell was confirmed to be ipRGC-driven by its photosensitivity in the presence of glutamate blockers. *B)* Mean±S.E.M. of all 20 cells tested (11 monostratified, 5 bistratified, 4 polyaxonal). *C)* The final-to-peak photoresponse amplitude ratio measured under three superfusion conditions. *, $p < 0.05$; **, $p < 0.01$. *D*) The averaged final-topeak photoresponse amplitude ratio measured from 45

ipRGCs (6 M1, 12 M2, 4 M3, 13 M4 and 10 M5) during superfusion with normal Ames' (ref. [11]). Stimulus intensity was 13.6 log photons cm^{-2} s^{-1} in all panels.